NJC Letter

Indium and indium-oxide nanoparticle or nanorod formation within functionalised ordered mesoporous silica†

Yannick Guari,[a] Katerina Soulantica,[b] Karine Philippot,[b] Chloé Thieuleux,[a] Ahmad Mehdi,[a] Catherine Reyé,[a] Bruno Chaudret*[b] and Robert J. P. Corriu*[a]

[a] *Laboratoire de Chimie Moléculaire et Organisation du Solide (CNRS UMR 5637), Université des Sciences et Techniques du Languedoc, Université de Montpellier II, Place E. Bataillon, F-34095, Montpellier cedex 5, France. Fax: +33 4 67 14 38 52E-mail: guari@univ-montp2.fr*

[b] *Laboratoire de Chimie de Coordination du CNRS, 205, route de Narbonne, F-31077, Toulouse cedex 04, France. Fax: +33 5 61 55 30 03E-mail: chaudret@lcc-toulouse.fr*

Received (in Montpellier, France) 10th March 2003, Accepted 12th May 2003
First published as an Advance Article on the web 9th June 2003

Organized mesoporous silica materials containing phosphonate groups have been used for controlling the growth of indium(0) nanoparticles or nanorods, which are converted to indium-oxide without modification of their size and shape.

Quantum size and surface effect properties of nanometer-scaled semiconductor and metal particles have been of considerable interest during the past two decades.[1] However, the preparation of such nanoparticles with a uniform size and shape and, moreover, their organization in 2 or 3 dimensions remain very challenging problems.[2,3] Both requirements can be met by synthesizing monodisperse particles capped with ligands that allow them to self-organize in 2 or 3 dimensions. This method has recently been used for the preparation of quantum dot nanoparticles and, by some of us, for the prepartion of nanoparticles of main group elements.[4,5] The drawback of this method concerns the stability of the nanomaterial, the self-organization being easily lost. Another attractive method is the growth of metal and semi-conductor nanoparticles within the pores of a regular mesoporous material.[6] The use of the regular channels of ordered mesoporous silica as matrices for the controlled growth of mono-,[7] bimetallic[8] or oxide[9] nanoparticles and nanorods[10] has been reported. In this case, the inorganic matrix acts as a template for the nanoparticles. For this purpose, it is necessary to control the growth within and not outside the pores of the matrix. Inclusion of ligands, which will selectively coordinate to the precursors and further to the nanoparticles, is an attractive way to control nanoparticle growth exclusively within the pores. Some of us have demonstrated the possibility to selectively functionalise the pores of regularly organised mesoporous materials.[11,12] We have previously shown that the hexagonal channels of thiol-functionalised mesoporous silica were effective hosts for the growth of gold nanoparticles.[13] Our strategy is based on the chemical complexation of previously reported organometallic precursors.[14,15] In this case, reduction under mild conditions affords gold(0) nanoparticles with a narrow size distribution directly correlated to the pore size distribution. Other research groups have also explored a similar approach using functionalised silica for nanoparticles[16] or nanorod[17] formation.

We consider here the preparation of indium nanoparticles and nanorods. Indium is a low melting point metal, which can easily be oxidised into indium oxide (In_2O_3). Thin films of this transparent n-type semiconducting oxide with a band gap of around 3.6 eV are known to exhibit luminescence[18] and gas sensing[19] properties. In addition, indium oxide nanofibers[20] and nanosized indium oxide particles dispersed within pores of non-organised mesoporous silica[21,22] have been reported to give photoluminescent materials. Here, we present the formation of indium nanoparticles within the pores of phosphonate-functionalised SBA-15 and MCM-41 type materials and their coalescence to indium nanorods. Oxidation of the as-obtained indium(0) nanometer scale objects gives indium oxide without modification of the initial size and shape.

Mesoporous silica containing phosphonic acid diethyl ester groups $(EtO)_2P(O)(CH_2)_3SiO_{1.5}/9{\cdot}SiO_2$ ^{A}**1** (SBA-15 type material)[12] and $(EtO)_2P(O)(CH_2)_3SiO_{1.5}/28{\cdot}SiO_2$ ^{B}**1** (MCM-41 type material) were prepared by the co-condensation route of trimethoxysilylpropyldiethylphosphonate with tetraethylorthosilicate (TEOS) in the presence of the structure-directing agents, respectively $[poly(ethylene\ oxide)]_{20}[poly(propylene\ oxide)]_{70}[poly(ethylene\ oxide)]_{20}$ (Pluronic 123) in acidic media or hexadecyltrimethylammonium bromide (CTAB) in basic media. Using such a method, the lipophilic part of trimethoxysilylpropyldiethylphosphonate (*i.e.*, propyldiethylphosphonate) will be located in the lipophilic core of the formed micelles during the sol-gel process. As a result, the phosphonate groups will be located exclusively within the pore channels of the as-obtained materials. The solids are named $^{x}N_{y}$ where ***x*** indicates the conditions for the synthesis of the solid, namely **A** in acidic media and **B** in basic media, ***N*** denotes the number given to the materials: **1** for materials not containing any indium, **2** for composite materials accommodating indium(0) nanoparticles and **3** for materials accommodating nanorods, while ***y*** indicates the reaction conditions used for the impregnation of indium, namely: **a** corresponding to a theoretical amount of 12.95 wt % of indium in a one-step impregnation treatment, **b** corresponding to a theoretical amount of 42.65 wt % of indium in a five-step impregnation treatment, and **c** corresponding to a theoretical amount of 42.65 wt % of indium in a one-step impregnation.

The organometallic precursor chosen, InCp,[23] decomposes spontaneously at room temperature in the presence of materials ^{A}**1** or ^{B}**1** to give materials named ^{A}**2**$_{a,b,c}$ and ^{B}**2**$_{a}$. When the decomposition of InCp is performed in toluene under reflux instead of room temperature, nanorod formation takes place within the channels of the host material. Material ^{A}**3**$_{c}$ is

† Electronic supplementary information (ESI) available: high angle powder X-ray diffraction pattern of ^{A}**2**$_{b}$/O_2, TEM images of ^{A}**2**$_{a}$, ^{A}**2**$_{b}$ and ^{A}**2**$_{c}$ and correlation between the pore diameter and the indium(0) nanoparticle size for ^{B}**2**$_{a}$. See: http://www.rsc.org/suppdata/nj/b3/b302867b/

Table 1 Some relevant characteristics for the mesoporous materials

Sample	Organic content[a] / mmol g^{-1}	Th./exp.[a] indium / wt%	S_{BET}/ m^2 g^{-1}	D_p[b] / Å	V_p/cm^3 g^{-1}	d_{100}/Å	Wall thickness[c] / Å
$^{A}\mathbf{1}$	0.96	0/0	671	70/62	0.99	103	49/57
$^{A}\mathbf{2_a}$	0.85	12.95/11.63	429	–	0.65	–	–
$^{A}\mathbf{2_b}$	0.63	42.65/28.72	250	–	0.41	–	–
$^{A}\mathbf{2_c}$	0.79	42.65/25.65	231	–	0.40	–	–
$^{A}\mathbf{3_c}$	0.73	42.65/31.75	235		0.38		
$^{B}\mathbf{1}$	0.51	0/0	1006	23/20	0.85	39	22/25
$^{B}\mathbf{2_a}$	0.54	12.95/11.50	977	–	0.51	–	–

[a a] Calculated from elemental analysis. [b b] Calculated from adsorption/desorption branches. [c c] Calculated from $a_0 - D_p$ [$a_0 = 2d_{100}/3^{(1/2)}$].

prepared in the latter conditions from material $^{A}\mathbf{1}$ using a one-step impregnation treatment. The preparation of materials $^{A}\mathbf{2_{a,b,c}}$, $^{B}\mathbf{2_a}$ and $^{A}\mathbf{3_c}$ is described in the experimental section. The amount of indium in the resulting materials $^{A}\mathbf{2_a}$ or $^{B}\mathbf{2_a}$ was established by elemental analysis (Table 1). In the case of material $^{A}\mathbf{2_b}$(Fig. 1), only 28.72% of indium was found while the expected quantity was of 42.65%. This is in agreement with the observation of some residual InCp precursor in the filtrate from the fourth and fifth impregnation treatments. The presence of residual organometallic precursor in the filtrate was also observed for the preparation of materials $^{A}\mathbf{2_c}$ and $^{A}\mathbf{3_c}$.

Pore-filling of the host material was monitored both by the decrease in BET surface area and pore volume when comparing materials **1** and **2** or **1** and **3** (Table 1). As observed previously,[13] a decrease in the intensity of the reflections is obtained for the powder X-ray diffraction patterns of materials **2** and **3** compared to materials **1**. Such an observation can be explained both by the similar contrasts induced by silica and indium[24] and by the random distribution of nanoparticles or nanorods, which would lower the periodicity.[25] TEM studies showed a narrow nanoparticle size distribution for materials **2** centred at 5.3 nm for $^{A}\mathbf{2_a}$ and 3.5 nm for $^{B}\mathbf{2_a}$, in agreement with the pore size of the host material, respectively 7.0/6.2 nm (adsorption/desorption branch) for $^{A}\mathbf{1}$ and 2.3/2.0 nm (adsorption/desorption branch) for $^{B}\mathbf{1}$. It is worth noting that egg-shaped nanoparticles are obtained for material $^{B}\mathbf{2_a}$ while in all other cases the nanoparticles obtained are spherical. The value of 3.5 nm corresponds to the smaller section of these particles. We propose that this shape results both from the relatively high concentration of indium present inside the channels and from the constraint induced by the pore size. In the case of material $^{A}\mathbf{1}$, the channels are larger, which explains the more isotropic shape of the nanoparticles.

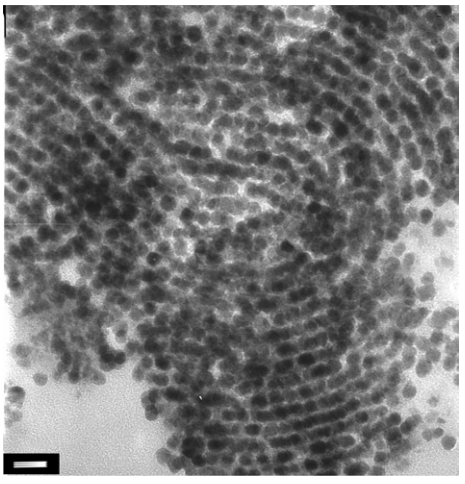

Fig. 1 TEM image of material $^{A}\mathbf{2_b}$. Scale bar = 20 nm.

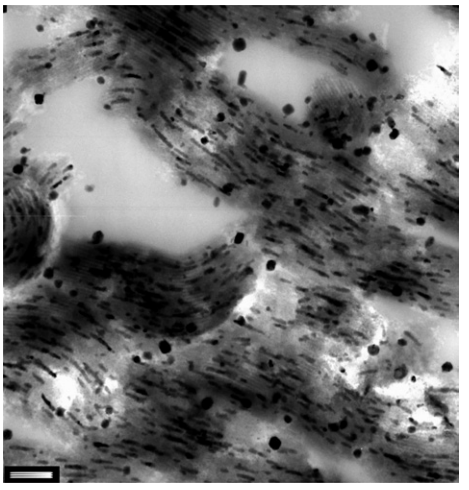

Fig. 2 TEM image of material $^{A}\mathbf{3c}$. Scale bar = 100 nm.

Small amounts of outer pore growth defects are visible for $^{A}\mathbf{2_b}$ and $^{A}\mathbf{2_c}$, leading to a size tail, which is substantially higher in the latter case. As observed by TEM studies for material $^{A}\mathbf{3_c}$ (Fig. 2), formation of nanoparticles and nanorods with lengths from 20 to 110 nm is observed within the pores, together with out-of-pore nanocrystallites of large size with a distribution centred at 285 nm. All our attempts to avoid crystallite growth outside the pores were unsuccessful. It has been previously proposed that the growth mechanism of nanorods could be related to the preferred coordination of the ligand along a face of a growing crystal.[26,27] In the present case, the coordination of the ligand to the crystal is dictated by the channel geometry of the matrix. This organisation leads to the presence of ligand-free crystal surfaces following the axis of the channel and allowing, under the conditions used, nanorod formation by the seed-mediated growth mechanism or, more likely, coalescence of nanoparticles in close proximity. The careful observation of Fig. 2 shows that indeed uniform nanorods form. However, in some cases, we can observe nanoparticles in close contact, which suggests that the coalescence mechanism is taking place as it was previously observed for the formation of indium[4] or ruthenium[28] nanowires.

When materials **2** and **3** are exposed to air, partial oxidation of the indium(0) nanoparticles or nanorods occurs as can be concluded from the powder XRD diffraction patterns. For material $^{A}\mathbf{2_b}$, the CP MAS ^{31}P NMR spectra display an enlarged signal at 33 ppm compared to the sharp signal observed for the free phosphonic acid diethylester group. This can be explained by the weak coordination of the organic functions to the nanoparticles. In order to confirm the coordinating role of the phosphonate groups, we performed the same experiments starting from non-functionalised SBA-15 mesoporous silica[29] instead of $^{A}\mathbf{1}$ or $^{B}\mathbf{1}$. For a material containing amounts of indium comparable to the indium weight within materials $^{A}\mathbf{2_a}$ or $^{B}\mathbf{2_a}$ as given by elemental analysis, we observed the growth of the indium(0) nanoparticles exclusively within the pores. However, for higher loadings, crystallites resulting from out-of-pore growth with a very large distribution centred at 180 nm were obtained, even with a five-step impregnation procedure as followed for $^{A}\mathbf{2_b}$, thus demonstrating the benefit of using functionalised silica.

Subsequently, materials **2** and **3** were oxidised under a constant dioxygen flow of 50 mL min^{-11}. The temperature was increased from room temperature to 353 K at a rate of 3 K min^{-1} and maintained for 1.5 h. Then, the temperature was increased to 473 K at a rate of 1 K min^{-1}. The resultant samples are designated $\mathbf{2/O_2}$ and $\mathbf{3/O_2}$. The powder XRD diffraction pattern of the resulting material $^{A}\mathbf{2_b/O_2}$ shows diffraction peaks indexed as (222), (400), (440) and (622) reflections of the

body-centred cubic structure of indium oxide.[30] TEM studies carried out on materials **2/O$_2$** and **3/O$_2$** clearly show that the size and shape of the nanometer scale objects are not affected by the thermal treatment under dioxygen atmosphere.

In summary, we describe for the first time the incorporation of indium within organised mesoporous hybrid materials allowing a good control of the size of the nanoparticles obtained. The exclusive formation of the particles inside the pore channels of the mesoporous material likely results from the coordination of the organometallic precursors to the ligands (*e.g.*, phosphonate) present in the mesoporous structure. Only when the channels are saturated with indium do we observe some out-of-pore growth. We also show that the oxidation of these nanoparticles to give indium oxide can be achieved without modification of their size and shape. Furthermore, by modifying the experimental conditions, indium nanorods were obtained and treated in the same way to give indium oxide nanorods. Applications of these nanometer scale objects in various fields including optics will be reported later.

Experimental

In a typical experiment, the incorporation of indium was done as follows. A solution of InCp (23.5 mg, 0.13 mmol.) in toluene (10 mL) was added to a suspension of ^{A}**1** or^{B}**1** (100 mg) in toluene (5 mL) at room temperature under argon and stirred overnight. The product was filtered off, rinsed with toluene and dried under vacuum to afford materials ^{A}**2**$_{a}$ or ^{B}**2**$_{a}$ as slightly grey powders. Similar treatment of material ^{A}**1** repeated five times led to material ^{A}**2**$_{b}$ as a black powder. The same quantity of InCp (117.5 mg, 0.75 mmol.) as in the last experiment was added in a one-step impregnation and led to material ^{A}**2**$_{c}$. A one-step impregnation with the same quantity of InCp at reflux in toluene led to material ^{A}**3**$_{c}$.

Acknowledgements

The authors thank the CNRS and the Université de Montpellier II for financial support. C. T. thanks Air Liquide for a grant.

References

1 A. P. Alivisatos, *Science*, 1996, **271**, 933; J. Shi, S. Gider, D. Babcock and D. D. Awschalom, *Science*, 1996, **271**, 937.
2 *Clusters and Colloids, from Theory to Applications*, ed. G. Schmid, VCH, Weinheim, 1994.
3 *Nanoparticles and Nanostructured Films, Preparation, Characterization and Applications*, ed. J. H. Fendler, VCH, Weinheim, 1998.
4 K. Soulantica, A. Maisonnat, F. Senocq, M.-C. Fromen, M.-J. Casanove, P. Lecante and B. Chaudret, *Angew. Chem., Int. Ed.*, 2001, **40**, 2984.
5 K. Soulantica, A. Maisonnat, M.-C. Fromen, M.-J. Casanove, P. Lecante and B. Chaudret, *Angew. Chem., Int. Ed.*, 2001, **40**, 448; F. Dumestre, B. Chaudret, C. Amiens, M.-C. Fromen, M.-J. Casanove, P. Renaud and P. Zurcher, *Angew. Chem., Int. Ed.*, 2002, **41**, 4286.
6 C. T. Kresge, M. E. Leonowicz, W. J. Roth, J. C. Vartuli and J. S. Beck, *Nature (London)*, 1992, **359**, 710.
7 Y. Plyuto, J.-M. Berquier, C. Jacquiod and C. Ricolleau, *Chem. Commun.*, 1999, 1653; P. Mukherjee, C. R. Patra, R. Kumar and M. Sastry, *Phys. Chem. Commun.*, 2001, 5; L. H. Bronstein, S. Polarz, B. Smarsly and M. Antonietti, *Adv. Mater.*, 2001, **13**, 1333; M. A. Aramendia, V. Borau, C. Jimenez, J. M. Marinas and F. J. Romero, *Chem. Commun.*, 1999, 873.
8 D. Ozkaya, W. Zhou, J. M. Thomas, P. Midgley, V. J. Keast and S. Hermans, *Catal. Lett.*, 1999, **60**, 113; F. Schweyer, P. Braunstein, C. Estournès, J. Guille, H. Kessler, H.-L. Paillaud and J. Rosé, *Chem. Commun.*, 2000, 1271.
9 Z. Y. Yuan, S. Q. Liu, T. H. Chen, J. Z. Wang and H. X. Li, *Chem. Commun.*, 1995, 973; M. Iwamoto, T. Abe and Y. Tachibana, *J. Mol. Catal. A: Chem.*, 2000, **155**, 143; R. Köhn and M. Fröba, *Catal. Today*, 2001, **68**, 227; R. S. Mulukutla, K. Asakura, S. Namba and Y. Iwasawa, *Chem. Commun.*, 1998, 1425.
10 X.-J. Han, J. M. Kim and G. D. Stucky, *Chem. Mater.*, 2000, **12**, 2068; M. H. Huang, A. Choudrey and P. Yang, *Chem. Commun.*, 2000, 1063; Z. Liu, Y. Sakamoto, T. Ohsuna, K. Hiroga, O. Terasaki, C. H. Ko, H. J. Shin and R. Ryoo, *Angew. Chem., Int. Ed.*, 2000, **39**, 3107; A. Fukuoka, Y. Sakamoto, S. Guan, S. Inagaki, N. Sugimoto, Y. Fukushima, K. Hirahara, S. Iijima and M. Ichidawa, *J. Am. Chem. Soc.*, 2001, **123**, 3373; H. Kang, Y.-W. Jun, J.-I. Park, K.-B. Lee and J. Cheon, *Chem. Mater.*, 2000, **12**, 3530.
11 R. J. P. Corriu, C. Hoarau, A. Mehdi and C. Reyé, *Chem. Commun.*, 2000, 71; R. J. P. Corriu, A. Mehdi and C. Reyé, *C. R. Acad. Sci., Ser. IIc: Chim.*, 1999, **2**, 35; R. J. P. Corriu, F. Embert, Y. Guari, A. Mehdi, C. Reyé and C. Thiuleux, *Chem. Commun.*, 2001, 1116.
12 R. J. P. Corriu, L. Datas, Y. Guari, A. Mehdi, C. Reyé and C. Thieuleux, *Chem. Commun.*, 2001, 763.
13 Y. Guari, C. Thieuleux, A. Mehdi, C. Reyé, R. J. P. Corriu, S. Gomez-Gallardo, K. Philippot, B. Chaudret and R. Dutartre, *Chem. Commun.*, 2001, 1374; Y. Guari, C. Thieuleux, A. Mehdi, C. Reyé, R. J. P. Corriu, S. Gomez-Gallardo, K. Philippot and B. Chaudret, *Chem. Mater.*, 2003, **15**, 2017.
14 J. Turkevitch, P. C. Stevenson and J. Hillier, *Discuss. Faraday Soc.*, 1951, **73**, 55.
15 S. Gomez, K. Philippot, V. Collière, B. Chaudret, F. Senocq and P. Lecante, *Chem. Commun.*, 2000, 1945; S. Gomez, L. Erades, K. Philippot, B. Chaudret, V. Collières, O. Balmes and J.-O. Bovin, *Chem. Commun.*, 2001, 1474.
16 H. Wellmann, J. Rathousky, M. Wark, A. Zukal and G. Schylz-Ekloff, *Microporous Mesoporous Mater.*, 2001, **44–45**, 419; C. R. Patra, A. Ghosh, P. Mukherjee, M. Sastry and R. Kumar, *Stud. Surf. Sci. Catal.*, 2002, **141**, 641; Y. S. Cho, J. C. Park, B. Lee, Y. Kim and J. Yi, *Catal. Lett.*, 2002, **81**, 89; C.-H. Yang, P.-H. Liu, Y.-F. Ho, C.-Y. Chiu and K.-J. Chao, *Chem. Mater.*, 2002, **15**, 275.
17 L.-X. Zhang, J.-L. Shi, J. Yu, Z.-L. Hua, X.-G. Zhao and M.-L. Ruon, *Adv. Mater.*, 2002, **14**, 1510; C.-M. Yang, H.-S. Sheu and K.-J. Chao, *Adv. Funct. Mater.*, 2002, **12**, 143.
18 M.-S. Lee, W. C. Choi, E. K. Kim, C. K. Kim and S.-K. Min, *Thin Solid Films*, 1996, **279**, 1.
19 A. Gurlo, M. Ivanovskaya, N. Bârsan, M. Schweizer-Berberich, U. Weimar, W. Göpel and A. Diéguez, *Sens. Actuators, B*, 1998, **44**, 327.
20 C. Liang, G. Meng, Y. Lei, F. Phillipp and L. Zhang, *Adv. Mater.*, 2001, **13**, 1330.
21 H. Zhou, W. Cai and L. Zhang, *Mater. Res. Bull.*, 1999, **34**, 845; H. Zhou, W. Cai and L. Zhang, *Appl. Phys. Lett.*, 1999, **75**, 495.
22 A. Murali, A. Barve, V. J. Leppert, S. H. Risbud, I. M. Kennedy and H. W. H. Lee, *Nano Lett.*, 2001, **1**, 287.
23 O. T. Beachley, Jr., J. C. Pazik, R. Z. Glassman, M. R. Churchill, J. C. Fettinger and R. Blom, *Organometallics*, 1998, **7**, 1051.
24 B. Marler, U. Oberhageman, S. Vortmann and H. Gies, *Microporous Mater.*, 1996, **6**, 375.
25 B. J. Aronson, C. F. Blanford and A. Stein, *J. Phys. Chem. B*, 2000, **104**, 449.
26 V. F. Puntes, K. M. Krishana and A. P. Alivisatos, *Appl. Phys. Lett.*, 2001, **78**, 2187; V. F. Puntes, K. M. Krishnan and A. P. Alivisatos, *Science*, 2001, **291**, 2115.
27 Z. A. Peng and X. Peng, *J. Am. Chem. Soc.*, 2001, **123**, 1389.
28 C. Pang, K. Pelzer, K. Philippot, B. Chaudret, F. Dassenoy, P. Lecante and M.-J. Casanove, *J. Am. Chem. Soc.*, 2001, **123**, 7584.
29 D. Zhao, J. Feng, Q. Huo, N. Melosh, G. H. Fredrickson, B. F. Chmelka and G. D. Stucky, *Science*, 1998, **279**, 548.
30 From the XRD diagram obtained, the space groups *Ia*-3 and *I*2$_1$3 could not be distinguished.